Available online at www.sciencedirect.com

ScienceDirect

Advances in Space Research 38 (2006) 1861–1869

ADVANCES IN SPACE RESEARCH
(a COSPAR publication)

www.elsevier.com/locate/asr

ERG – A small-satellite mission to investigate the dynamics of the inner magnetosphere

K. Shiokawa [a,*], K. Seki [a], Y. Miyoshi [a], A. Ieda [a], T. Ono [b], M. Iizima [b], T. Nagatsuma [c], T. Obara [c], T. Takashima [d], K. Asamura [d], Y. Kasaba [d], A. Matsuoka [d], Y. Saito [d], H. Saito [d], M. Hirahara [e], Y. Tonegawa [f], F. Toyama [f], M. Tanaka [f], M. Nose [g], Y. Kasahara [h], K. Yumoto [i], H. Kawano [i], A. Yoshikawa [i], Y. Ebihara [j], A. Yukimatsu [j], N. Sato [j], S. Watanabe [k], the Inner Magnetosphere Subgroup in the Society of Geomagnetism and Earth, Planetary and Space Sciences

[a] *Solar–Terrestrial Environment Laboratory, Nagoya University, Toyokawa 442-8507, Japan*
[b] *Graduate School of Science, Tohoku University, Sendai 980-8578, Japan*
[c] *National Institute of Information and Communications Technology, Koganei, Tokyo 184-8795, Japan*
[d] *Institute of Space and Astronautical Science, Japan Aerospace Exploration Agency, Sagamihara 229-8510, Japan*
[e] *Faculty of Science, Rikkyo University, Toshima-ku, Tokyo 171-8501, Japan*
[f] *Faculty of Engineering, Tokai University, Hiratsuka 259-1292, Japan*
[g] *Faculty of Science, Kyoto University, Sakyo-ku, Kyoto 606-8502, Japan*
[h] *Faculty of Engineering, Kanazawa University, Kanazawa 920-8667, Japan*
[i] *Faculty of Science, Kyushu University, Fukuoka 812-8581, Japan*
[j] *National Institute of Polar Research, Itabashi-ku, Tokyo 173-8515, Japan*
[k] *Graduate School of Science, Hokkaido University, Sapporo 060-0810, Japan*

Received 1 November 2004; received in revised form 3 May 2005; accepted 15 May 2005

Abstract

The Earth's inner magnetosphere (inside 10 Re) is a region where particle energy increases to the relativistic energy range. This region is very important as a laboratory where high-energy particle acceleration can be directly measured in a dipolar field configuration, as well as for human activities in space including space weather prediction. Despite abundant in situ satellite measurements, this region has been "missing" because of several difficulties arising from the measurements, such as high-energy particle contamination of low-energy particle measurement, protection against the possible incidence of radiation belt particles on the satellite, and the difficulties of measuring three-dimensional particles over a broad energy range, from a few electron volts to more than 10 MeV. In this paper, we address important scientific topics and propose a possible configuration of small satellites termed Energization and Radiation in Geospace (ERG), which would provide new insights into the dynamics of the inner magnetosphere and strongly contribute to the International Living With a Star project.

Keywords: Inner magnetosphere; Small satellite mission; Magnetic storm; Radiation belt

1. Introduction

The Earth's inner magnetosphere (inside 10 Re) has been a "missing" region in terms of scientific investiga-

---

[*] Corresponding author.
E-mail address: Shiokawa@stelab.nagoya-u.ac.jp (K. Shiokawa).

0273-1177/$30
doi:10.1016/j.asr.2005.05.089

tion, particularly in the area of plasma dynamics. This is because there have been few satellites that simultaneously measure magnetic and electric fields and plasma moments and composition over a broad energy range in the inner magnetosphere near the equatorial plane. Intense radiation-belt particles often prevent the satellites to be operated in the inner magnetosphere. Such an inner magnetospheric satellite mission would unveil the principal mechanisms of energy flow from the magnetosphere to the ionosphere.

Since April 2001, young scientists have been gathering at the monthly ‘‘Discussion for Future’’ meetings, held at the Tokyo Institute of Technology, to discuss future missions of magnetospheric research satellites. Two major missions have been the main subjects of discussion: (1) the so-called SCOPE mission, which investigates reconnection regions, shock and boundary layers, with high-time-resolution multisatellites, and (2) the inner magnetospheric mission, which uses relatively small satellite(s). For the latter mission, the Inner Magnetosphere Subgroup was newly established in the Society of Geomagnetism and Earth, Planetary and Space Sciences, Japan, on November 14, 2002. The numbers of local meetings and workshops related to this topic were 3 (2001), 12 (2002), 4 (2003), and 6 (2004). Based on the discussions at these meetings, we are proposing a small-satellite mission termed Energization and Radiation in Geospace (ERG) to the Japan Aerospace Exploration Agency. In this paper, we describe the current status of knowledge of the inner magnetosphere, as well as problems that can be investigated by this new mission.

The subjects are: (1) radiation belt dynamics, (2) ring current dynamics, (3) substorm dynamics and energetics, (4) ULF waves, (5) plasma waves, and (6) mass transport, including heavy ions. We also briefly describe strategies and possible configurations of the ERG mission.

2. Scientific subjects

2.1. Radiation belt dynamics

The radiation belt particles have the highest energy of the plasmas in the terrestrial magnetosphere. Recent observations by CRRES, SAMPEX, NOAA, Akebono and Tsubasa revealed that the radiation belt particles, particularly relativistic electrons in the outer belt, vary significantly during magnetic storms. The investigation of such dynamic behavior is very important, both for understanding general acceleration processes of particles in the dipolar magnetic field of planets and stars, and for applications to the prediction of space weather.

There are two major questions regarding the dynamic behavior of the relativistic electrons in the outer radiation belt: the sudden disappearance of the relativistic electrons during the main phase of the storm, and acceleration of the relativistic electrons during the storm recovery phase (e.g., Nagai, 1988; Obara et al., 2001). An example of such dynamic behavior observed by NOAA and Akebono is shown in Fig. 1 (after Miyoshi et al., 2003). The high energy electron fluxes decrease at day 308 during the main phase of the storm. Then the electron fluxes significantly increase during the recovery phase of the storm particularly after day 309. The flux enhancement exceeds the pre-storm flux level, indicating that particle acceleration does occur during the recovery phase of the storm.

The disappearance of the relativistic electrons during the main phase is generally explained by the adiabatic effect, which is due to depletion of the ambient magnetic field by enhanced ring current. However, the loss of the relativistic electrons often exceeds the loss expected from the adiabatic effect. Other mechanisms that are candidates for explaining the loss of relativistic electrons during the storm's main phase are: (1) precipitation into the atmosphere due to pitch-angle scattering by both the whistler-mode waves and the electromagnetic ion cyclotron (EMIC) waves (e.g., Horne and Thorne, 1998), and (2) loss to the magnetopause due to the drift motion of the relativistic electrons (e.g., Desorgher et al., 2000). To reach a definitive conclusion about the loss mechanism of the relativistic electrons, it is essential to re-

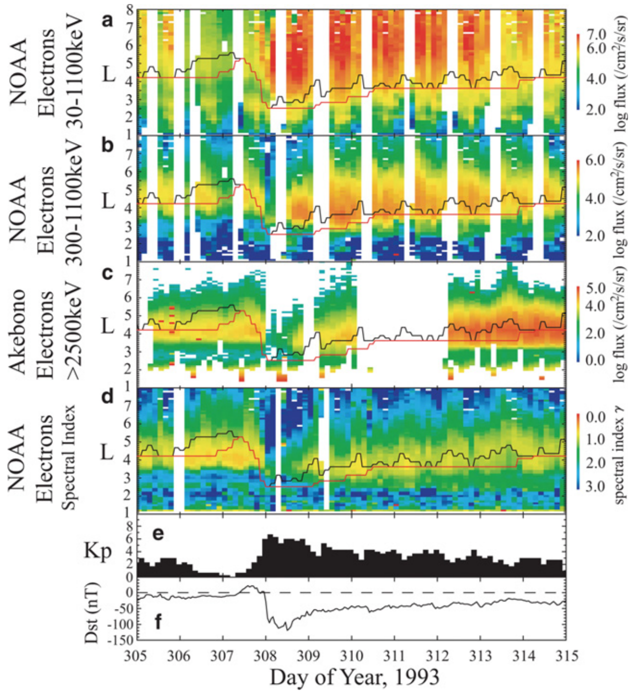

Fig. 1. Dynamic behaviour of the outer radiation belt observed by NOAA and Akebono (low altitude satellites) during the November 3, 1993, storm (after Miyoshi et al., 2003). The red and black curves in each panel indicate empirical plasmapause location and convection limit, respectively.

move the adiabatic effect by measuring the local magnetic field and the electron flux near the equatorial plane.

The rapid recovery and enhancement of the outer radiation belt during the storm recovery phase is the most remarkable feature of the relativistic electron behavior. The flux recovery is basically associated with the recovery of ambient magnetic field intensity (an adiabatic process). As in the example shown in Fig. 1, however, the accelerated electron flux often exceeds the pre-storm level, indicating that some additional mechanisms come into play. The models for the acceleration of relativistic electrons during the storm recovery phase are:

(1) Supply from the outside (adiabatic): Relativistic electrons may be supplied from outside the radiation belts due to enhanced radial diffusion and substorm injection of electrons. This process is basically adiabatic process, and the Pc 5 magnetic pulsation has been considered to be plausible candidate for driver of enhanced radial diffusion (e.g., Li et al., 1997; Elkington et al., 1999; Tan et al., 2004).
(2) Internal acceleration (non-adiabatic): Several non-adiabatic processes, which can accelerate electrons to relativistic energy inside the radiation belts, are proposed. (a) Wave–particle interaction with whistler mode waves (e.g., Summers and Ma, 2000a; Miyoshi et al., 2003) and Pc 4 and Pc 5 pulsations (e.g., Summers and Ma, 2000b), (b) recirculation process (Fujimoto and Nishida, 1990; Liu et al., 1999). If these processes work during magnetic storms, the phase space density (PSD) should have significant crest structure inside the inner magnetosphere.

In order to separate the processes outside the radiation belts (1) from internal accelerations (2), it is essential to determine which part (outside or inside) of the electron PSD first increases during the recovery phase, based on measurement of radial profile of PSD. Currently, it is difficult to determine the PSD profile because of the lack of observations at the equatorial plane. Construction of a reliable storm-time magnetic field model will be also important for this study. Furthermore, to separate different acceleration/diffusion mechanisms, it will be necessary to measure: (1) the plasma wave amplitude and wavenumber spectra in the equatorial plane to estimate the acceleration by plasma waves quantitatively, (2) the distribution of seed electrons (eV and keV energy electrons), (3) thermal plasma density (including locations relative to the plasmapause) that determines the resonance condition of wave–particle interactions, and (4) the phase and amplitude of ULF waves. It is also important to develop ambient magnetic and electric field models, particularly in the equatorial plane. To study interactions between relativistic electrons and plasma/ULF waves, a comparison with model calculations will be needed. Thus, the development of comprehensive physical model of the inner magnetosphere would be very important for the ERG project.

2.2. *Ring current dynamics*

In the inner magnetosphere, the dynamic behavior of plasma energy density is dominated by ions with energies of 1–200 keV. Such ions are a key to understand the dynamics of the inner magnetosphere, because an intense ring current is carried by the ions, causing the *Dst* variation and driving the Region 2 field-aligned currents to couple with the ionosphere. The growth and decay of the plasma energy density (ring current) are traditionally monitored by ground magnetograms at low- and mid-latitudes as the *Dst* index. One can roughly estimate the total energy stored in the inner magnetosphere from the *Dst* variation. However, the *Dst* index does not resolve any spatial distribution of the energy density. An in situ satellite measurement gives us helpful information on the ring current, but the data is hardly distinguishable between temporal and spatial changes. An imaging technique has been recently used by the IMAGE satellite (Burch, 2000), providing capability to take a global picture of the ring current. However, a line-of-sight measurement is accompanied by ambiguities arising from the inversion problem. Under this circumstance, multisatellite observations with a broad energy range are essential to understand the structure and dynamics of the ring current. In addition, ion measurements with a broad energy range (between tens of eV and MeV) for different ionic species are necessary to understand transport and energization processes of the ring current ions, because ions drifting inward from $L = 10$ to $L = 2$ are adiabatically accelerated to an energy hundreds of times higher than that at the original location.

Recent observations of the electric and magnetic fields have revealed the fact that the electric and magnetic fields in the inner magnetosphere have much more complicated structure than thought before. On the basis of data from the CRRES satellite, Rowland and Wygant (1998) have shown that the large-scale electric field tends to show a localized enhancement on the duskside as increased K_p, indicating that a traditional model, e.g., the Volland–Stern type convection electric field model, fails to explain the observation. In addition, strong stretching of the magnetic field down to $L < 4$ was observed during the storm main phase at all local times (Korth et al., 2000). All these observational results imply that the behavior of the ring current ions should not be simple as predicted before.

Numerical simulation is a powerful and unique tool for making up for the weak points of the observations, and for testing possible mechanisms that account for observations. Recent simulations are capable of explaining storm-time *Dst* variation to the zeroth-order approximation when they use an empirical magnetic and electric fields (e.g., Ebihara and Ejiri, 2000). However, one sometimes encounters a problem in explaining behavior of the storm-time differential flux of the ring current ions, even though the simulated *Dst* fairly agrees with the observed one (e.g., Jordanova et al., 1999; Liemohn et al., 2001). This disagreement poses a question on the physical meaning of the *Dst* and its relationship to the ring current.

The following long-standing questions are expected to be solved by performing multisatellite observations acquired with multi-ionic species and a broad energy range (tens of eV to MeV) as well as simultaneous observations of DC and AC magnetic and electric fields. (1) Post-midnight enhancement of the ring current ion fluxes (C:son Brandt et al., 2002): A numerical simulation performed with a previously existing convection electric field model shows that the peak of the energy density occurs in the dusk–midnight sector. However, the statistical distribution of the energy density measured by in situ observation shows that the peak of energy density occurs near midnight (Ebihara et al., 2002). ENA images of the ring current protons show that the peak of the flux sometimes occurs in the post-midnight sector (C:son Brandt et al., 2002). This challenges conventional wisdom. (2) Generation mechanism of the high-energy component of the ring current (>100 keV): The high-energy component is observed to be weakened during a main phase, and enhanced during a recovery phase. This behavior is not simply attributed to the convection electric field. (3) Isotropic pitch-angle distribution: Data from low-altitude satellites (NOAA) shows that the loss cone of ions with energies of tens of keV is filled above a certain latitude. Kozyra et al. (1998) have pointed out that the isotropic precipitation is important for explaining the rapid recovery of the ring current as well as the charge exchange. One of the possible mechanisms is stochastic motion of the ion in the region where the gyroradius is larger than the radius of the curvature of a field line. However, no evidence is yet presented by performing direct observations of the stochastic motion near the equatorial plane, where the ratio between the gyroradius and the radius of the curvature of a field line is small. (4) Contribution from electrons to the ring current: Frank (1967) has shown that contribution from electrons to *Dst* is estimated to be 20 % of the ion energy density. Data from Explorer 45 shows that contribution from electrons becomes comparable to that from ions at certain *L*, indicating that the electron ring current should not be negligible (Ejiri et al., 1977). (5) Formation of broadband electrons and their relation to the mid-latitude red aurora: Shiokawa et al. (1996) found using the DMSP satellite data that electrons with broad energy range from 30 eV to 30 keV precipitated in the subauroral zone at ∼50–60° MLAT associated with storm-time substorms. These electrons can be a cause of red auroras observed at mid-latitudes (Shiokawa et al., 1997). Simultaneous CRRES data show turbulent magnetic and electric field and energization of parallel electrons in the source region of the broadband electrons at $L = 6$ (Shiokawa et al., 1999). However, the mechanism that produces such electrons is still unknown.

2.3. Substorm dynamics and energetics

Substorms are the basic process for releasing the energy stored in the magnetotail into the near-Earth dipolar-field region. The magnetic field energy stored as the lobe magnetic flux during the growth phase is carried Earthward through reconnection and finally dissipated into the ionosphere in the dipolar field region. The inner magnetosphere is the main region where the substorm energy is converted into the ionosphere for dissipation (e.g., Haerendel, 2000). Lui (2003) recently compiled the pressure profile obtained by the AMPTE/CCE satellite according to the K_p index. Such measurements of plasma and magnetic pressures according to the substorm phases are essential to solve the role of the inner magnetosphere in substorm energy dissipation to the ionosphere.

Substorm onset processes, particularly those of the first few minutes, are still controversial. There are two major models of the cause of the initial onset of substorms. One is the near-Earth neutral line (NENL) model, based on the spontaneous reconnection at 20–30 Re (e.g., Baker et al., 1996; Shiokawa et al., 1998), while the other is the current disruption and/or reduction of pressure gradient in the inner magnetosphere inside 10 Re (e.g., Lui, 1991; Lyons, 1995). To clarify the latter model, it is essential to make systematic (long-term) observations of three-dimensional plasma distribution and magnetic and electric fields, particularly in the inner magnetosphere near the equatorial plane. The inner magnetospheric satellite mission will give us the core data set for investigating this subject.

2.4. ULF waves

The inner magnetosphere plays an important role in the selection of particular frequencies of MHD waves from disturbances in the outer magnetosphere and the solar wind, and produces several characteristics of ULF waves. This is because the magnetic field rapidly changes from tail-like to a dipolar shape in the inner magnetosphere to allow field-line resonance. The other reason is the existence of the plasmapause, where the Alfvén velocity suddenly changes to form a boundary of wave propagation and cavity mode oscillations. The processes of frequency selection and the formation of various wave modes, however, are still unclear and controversial.

For example, Pi 2 magnetic pulsations have a period of 40–150 s and are a sensitive indicator of substorm onset. Signatures of high-latitude Pi 2 in the auroral zone and low latitude Pi 2 are different (e.g., Yumoto and CPMN group, 2001), probably corresponding to the difference in the wave modes inside and outside the plasmasphere. Various models are proposed for the Pi 2 mechanisms, such as oscillations of auroral field-aligned current, field-line resonance, plasmaspheric cavity-mode oscillations, and so on (see Olson, 1991, for a review). Recently, Kepko and Kivelson (1999) proposed that the oscillation of bursty bulk flow in the tail directly drives Pi 2 oscillations. Takahashi et al. (2001) discuss Pi 2 modes using magnetic and electric field data obtained by the CRRES satellite in the inner magnetosphere. They show that the electric and magnetic field data are useful for identifying the wave modes, not only for the Pi 2 pulsations but also for other ULF waves in the inner magnetosphere.

Continuous electric and magnetic field measurements are essential for determining the various ULF modes in the inner magnetosphere. These data also allow us to estimate the Poynting flux of the waves, which indicates the AC component of the magnetic energy flow from the magnetosphere to the ionosphere. Simultaneous observations inside and outside the plasmasphere near the equatorial plane will be important for identifying mode conversion processes at the plasmapause.

2.5. Plasma waves

The 14 years of wave measurements by the Akebono satellite have identified various types of plasma waves inside the plasmasphere, indicating that like the outer magnetosphere, the plasmasphere is an active region of plasma waves. These waves are mostly observed near the equatorial plane, even in the magnetically quiet interval, as shown in Fig. 2. The plasma wave indicated as EPWAT in Fig. 2 is the enhancement of wave intensity in a frequency range from UHR to the Z-mode cutoff frequency and is confined to a narrow latitude range near the equatorial plane (Oya et al., 1991). EPWAT probably corresponds to pitch-angle anisotropy of drifting electrons (1–10 keV). It is still unclear why EPWAT is localized in the equatorial plane. The electrostatic electron cyclotron harmonic waves at the f_{Qn} branch (named EP-ESCH in Fig. 2) are also observed in the equatorial region and probably indicate temperature anisotropy at an energy of a few tens of eV. However, due to technical problems, the velocity distribution function of suprathermal electrons in this region has not been measured simultaneously with these plasma waves.

During the recovery phase of magnetic storms, the variation in UHR frequency measured along the Akebono satellite orbit often revealed a ‘‘donkey-ear type’’ profile (Oya, 1991). The phenomenon is due to the formation of a density depletion region inside the plasmasphere and may be related to a ‘‘plasma void,’’ which was recently reported by the IMAGE satellite (Sandel

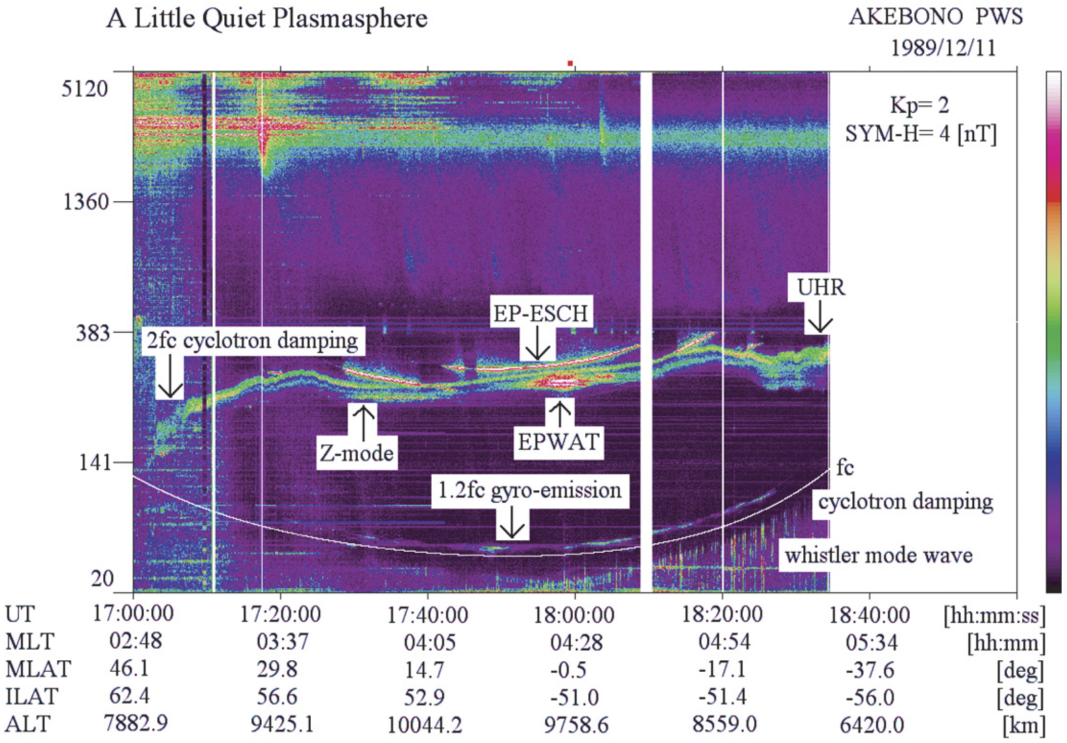

Fig. 2. Example of plasma waves observed by the Akebono satellite during a magnetically quiet interval on December 11, 1989.

et al., 2001). In discussing the formation of the donkey-ear phenomenon, Oya (1997) pointed out the importance of betatron drift due to the magnetic field fluctuation during magnetic storms. Simultaneous measurements of the electric and magnetic field, as well as plasma, will be needed to clarify this mechanism.

Associated with the storm-time disturbed state of the plasmasphere, intense R-X mode kilometric radiation is often observable, which cannot be explained by previous theories of cyclotron-maser or mode conversion mechanisms. This R-X mode radiation suggests some unknown mechanism of plasma wave generation in the storm-time inner magnetosphere.

2.6. Mass transport including heavy ions

In the inner magnetosphere, the oxygen ions originating from the Earth's atmosphere distribute in the ring current (high-energy ions) and the plasmasphere (low-energy ions). The ratio of heavy ions in the ring current drastically increases during magnetic storms and active times (e.g., Daglis, 1997). The source of this energetic oxygen is considered to be the magnetotail, ionosphere, and some local acceleration/heating in the inner magnetosphere. Measurement of the three-dimensional distributions of each ion species for a broad energy range, from eV to MeV, would allow a quantitative assessment of this subject. In the plasmasphere, Craven et al. (1997) have shown, using data from the DE 1 satellite, that the low-energy helium and oxygen ions have a correlation with radial distance and solar EUV flux. However, there has been no such measurement near the equatorial plane. These low-energy heavy ions can be the seeds of the above energetic ions in the inner magnetosphere.

3. Mission strategies

In the previous section, we reviewed the current status and unsolved scientific problems of the inner magnetosphere. On the basis of these discussions, we made a rough assessment of possible instruments and options for various scientific objectives. Fig. 3 summarizes the assessment. The scientific topics discussed in the previous sections are summarized in the left column. Possible instrumentations and measurement options are shown in the top line. From Fig. 3, the important features of the ERG mission can be summarized as: (1) simultaneous measurements of three-dimensional plasma distributions over a broad energy range from eV to MeV, electric and magnetic fields, and plasma waves, (2) measurements near the equatorial plane (inclination less than 10°), (3) a long lifetime and high data coverage, (4) coordination with other satellite measurements, (5) coordination with ground network measurements, and (6) comparison with model calculations.

Here we show strategies of the ERG mission on the basis of these features, by taking an example of the acceleration mechanisms of relativistic electrons in the radiation belts discussed in Section 2.1. The following five strategies can be considered.

1. Accurate measurements of particle phase space density (PSD): PSD is a key to identify the acceleration mechanism of radiation belt particles. Adiabatic particle acceleration by Earthward injection causes PSD increase from outside of the radiation belt. Non-adiabatic insitu acceleration predicts PSD increase from inside. The accurate PSD estimation requires measurements of both magnetic field intensity and particle distribution over a wide energy range near the equatorial plane at low inclinations.
2. Sensitive magnetic field measurements and particle measurements over a broad energy range from ~10 eV to 10 MeV: One of the non-adiabatic acceleration mechanisms of relativistic electrons is the interaction with whistler-mode waves occurring just outside the plasmasphere. A highly-sensitive search-coil magnetometer to detect magnetic field component of the whistler waves can identify the propagation mode of the whistler waves. The whistler waves are generated by keV-order electrons, and possibly accelerate electrons with energies of hundreds keV. The measurements of particle distribution over a broad energy range from eV to 10 MeV provides both generation of the waves and their acceleration of particles.
3. Coordination with ground network measurements: The other important acceleration mechanism of relativistic electrons is the interaction with ULF waves. Ground network observations of magnetometers and radars provide global distribution of ULF waves and background fields. Coordination of the ground network and the ERG satellite allows quantitative estimation of the particle acceleration by ULF waves.
4. Determination of upper limit energy of relativistic electrons: The upper limit of the particle acceleration energy also gives useful information to identify acceleration mechanisms. The high-energy particle detectors up to 10 MeV with sufficient energy resolution determines the highest energy of particular acceleration events, such as those associated with storm sudden commencement.
5. Development of connecting tools of various measurements: Coordinated measurements by ERG, other satellites, and ground networks should be connected by some tools based on global modeling codes, which include particle and fluid dynamics in the inner magnetosphere. Development of such modeling tools provides a new methodology of data handling to understand the global and dynamical particle acceleration mechanisms during magnetic storms.

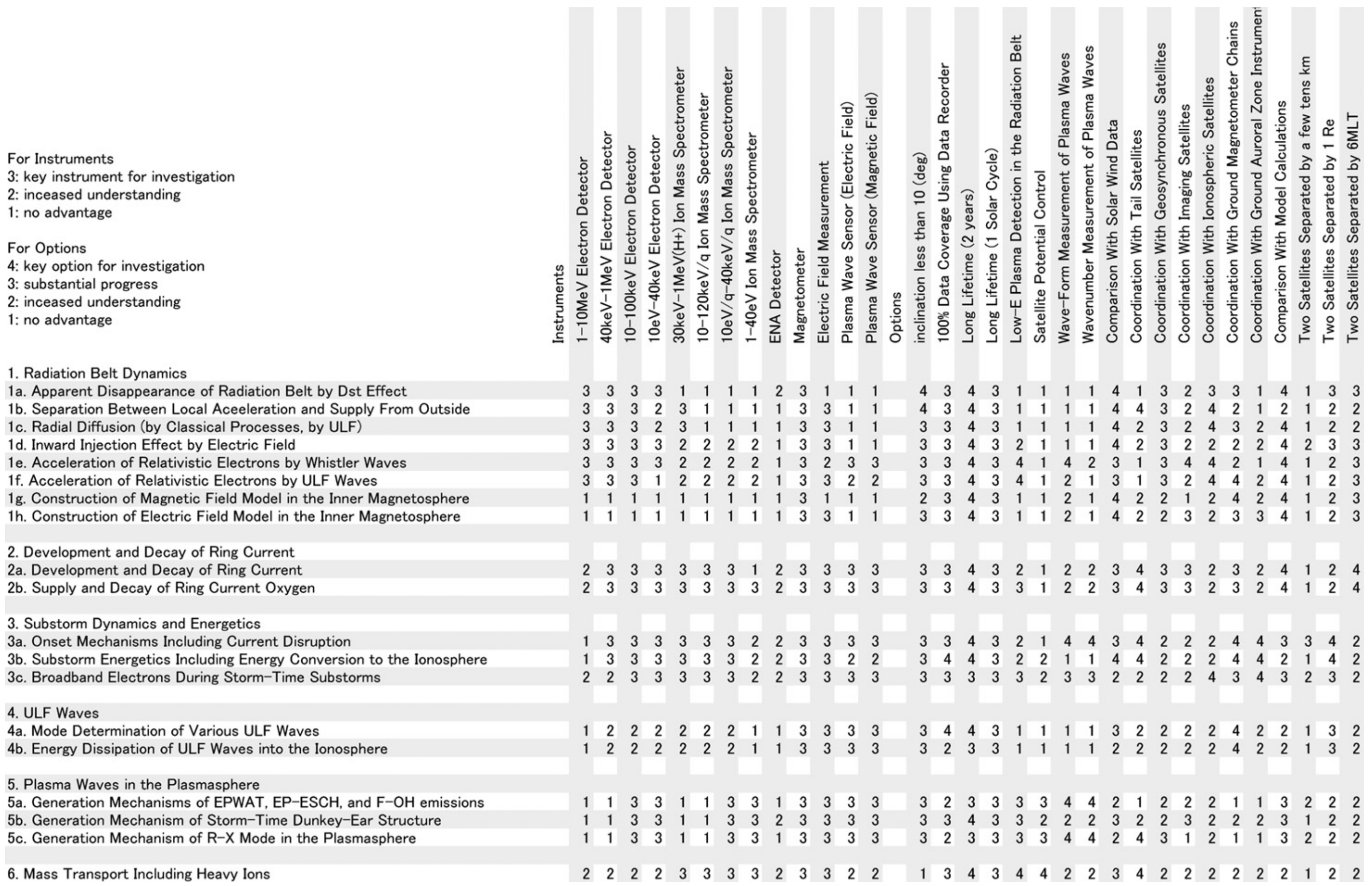

For Instruments
3: key instrument for investigation
2: inceased understanding
1: no advantage

For Options
4: key option for investigation
3: substantial progress
2: inceased understanding
1: no advantage

	Instruments	1–10MeV Electron Detector	40keV–1MeV Electron Detector	10–100keV Electron Detector	10eV–40keV Electron Detector	30keV–1MeV(H+) Ion Mass Spectrometer	10–120keV/q Ion Mass Spectrometer	10eV/q–40keV/q Ion Mass Spectrometer	1–40eV Ion Mass Spectrometer	ENA Detector	Magnetometer	Electric Field Measurement	Plasma Wave Sensor (Electric Field)	Plasma Wave Sensor (Magnetic Field)	Options	inclination less than 10 (deg)	100% Data Coverage Using Data Recorder	Long Lifetime (2 years)	Long Lifetime (1 Solar Cycle)	Low–E Plasma Detection in the Radiation Belt	Satellite Potential Control	Wave–Form Measurement of Plasma Waves	Wavenumber Measurement of Plasma Waves	Comparison With Solar Wind Data	Coordination With Tail Satellites	Coordination With Geosynchronous Satellites	Coordination With Imaging Satellites	Coordination With Ionospheric Satellites	Coordination With Ground Magnetometer Chains	Coordination With Ground Auroral Zone Instrumen	Comparison With Model Calculations	Two Satellites Separated by a few tens km	Two Satellites Separated by 1 Re	Two Satellites Separated by 6MLT
1. Radiation Belt Dynamics																																		
1a. Apparent Disappearance of Radiation Belt by Dst Effect		3	3	3	3	1	1	1	1	2	3	1	1	1		4	3	4	3	1	1	1	1	4	1	3	2	3	3	1	4	1	3	3
1b. Separation Between Local Aceeleration and Supply From Outside		3	3	3	2	3	1	1	1	1	3	3	1	1		4	3	4	3	1	1	1	1	4	4	3	2	4	2	1	2	1	2	2
1c. Radial Diffusion (by Classical Processes, by ULF)		3	3	3	2	3	1	1	1	1	3	3	1	1		3	3	4	3	1	1	1	1	4	2	3	2	4	3	2	4	1	2	2
1d. Inward Injection Effect by Electric Field		3	3	3	3	2	2	2	2	1	3	3	1	1		3	3	4	3	2	1	1	1	4	2	3	2	2	2	2	4	2	3	3
1e. Acceleration of Relativistic Electrons by Whistler Waves		3	3	3	3	2	2	2	2	1	3	2	3	3		3	3	4	3	4	1	4	2	3	1	3	4	4	2	1	4	1	2	3
1f. Acceleration of Relativistic Electrons by ULF Waves		3	3	3	1	2	2	2	2	1	3	3	2	2		3	3	4	3	4	1	2	1	3	1	3	2	4	4	2	4	1	2	3
1g. Construction of Magnetic Field Model in the Inner Magnetosphere		1	1	1	1	1	1	1	1	1	3	1	1	1		2	3	4	3	1	1	2	1	4	2	2	1	2	4	2	4	1	2	3
1h. Construction of Electric Field Model in the Inner Magnetosphere		1	1	1	1	1	1	1	1	1	3	3	1	1		3	3	4	3	1	1	2	1	4	2	2	3	2	3	3	4	1	2	3
2. Development and Decay of Ring Current																																		
2a. Development and Decay of Ring Current		2	3	3	3	3	3	3	1	2	3	3	3	3		3	3	4	3	2	1	2	2	3	4	3	3	2	3	2	4	1	2	4
2b. Supply and Decay of Ring Current Oxygen		2	3	3	3	3	3	3	3	2	3	3	3	3		3	3	4	3	3	1	2	2	3	4	3	3	2	3	2	4	1	2	4
3. Substorm Dynamics and Energetics																																		
3a. Onset Mechanisms Including Current Disruption		1	3	3	3	3	3	3	2	2	3	3	3	3		3	3	4	3	2	1	4	4	3	4	2	2	2	4	4	3	3	4	2
3b. Substorm Energetics Including Energy Conversion to the Ionosphere		1	3	3	3	3	3	3	2	2	3	3	2	2		3	4	4	3	2	2	1	1	4	4	2	2	2	4	4	2	1	4	2
3c. Broadband Electrons During Storm–Time Substorms		2	2	3	3	3	3	3	2	2	3	3	3	3		3	3	3	3	3	2	3	3	2	2	2	2	4	3	4	3	2	3	2
4. ULF Waves																																		
4a. Mode Determination of Various ULF Waves		1	2	2	2	2	2	2	1	1	3	3	3	3		3	4	4	3	1	1	1	1	3	2	2	2	2	4	2	2	1	3	2
4b. Energy Dissipation of ULF Waves into the Ionosphere		1	2	2	2	2	2	2	1	1	3	3	3	3		3	2	3	3	1	1	1	1	2	2	2	2	2	4	2	2	1	3	2
5. Plasma Waves in the Plasmasphere																																		
5a. Generation Mechanisms of EPWAT, EP–ESCH, and F–OH emissions		1	1	3	3	1	1	3	3	1	3	3	3	3		3	2	3	3	3	3	4	4	2	1	2	2	2	1	1	3	2	2	2
5b. Generation Mechanism of Storm–Time Dunkey–Ear Structure		1	1	3	3	1	1	3	3	2	3	3	3	3		3	3	4	3	3	2	2	2	3	2	2	3	2	2	2	3	1	2	2
5c. Generation Mechanism of R–X Mode in the Plasmasphere		1	1	3	3	1	1	3	3	1	3	3	3	3		3	2	3	3	3	3	4	4	2	4	3	1	2	1	1	3	2	2	2
6. Mass Transport Including Heavy Ions		2	2	2	2	3	3	3	3	2	3	3	2	2		1	3	4	3	4	4	2	2	3	4	2	2	2	2	2	2	1	2	2

Fig. 3. Assessment of possible instruments and options of the ERG mission for various scientific objectives.

In addition to the above strategies, simultaneous measurements with other satellites will be also important to the ERG mission. The environment of high energy particles and magnetic field disturbances has been continuously monitored by NOAA, LANL, and GOES satellites by the United States at low-Earth and geostationary orbits. Combining the comprehensive ERG dataset with these monitoring data will increase the understanding of the particle acceleration processes on global scale.

During the next solar maximum period of around 2011, NASA is planning to launch Living with a Star (LWS) satellites, which contains two Radiation Belt Storm Probe (RBSP) satellites in the equatorial plane of the inner magnetosphere. Canadian Space Agency is also planning to launch the ORBITALS satellite in the equatorial plane of the inner magnetosphere. These satellites has quite similar orbit to that of ERG (described in the following section). Placing these satellites at different longitudinal sectors will significantly contribute to the understanding of the high-energy particle acceleration processes, because high-energy particles are accelerated during their azimuthal drift motion around the Earth with periods from tens of minutes to hours.

4. Possible mission description

Based on the assessments and strategies described in the previous section, we propose a small-satellite mission termed ERG to investigate the dynamics of the inner magnetosphere. The details of the mission are shown in Fig. 4. The launch of the satellites will be around 2011, because it is in the next solar maximum period, and the LWS-RBSP and ORBITALS satellites are planned to be launched around this time, giving better longitudinal coverage to measure azimuthally drifting particles. The orbit will be elliptical, with a perigee of 250 km and an apogee of 6.6 Re. Such an elliptical orbit has an orbital period of ∼10 h and provides radial distributions of parameters with a time resolution of ∼5 h. The radial distribution of PSD is important to distinguish the adiabatic and non-adiabatic acceleration mechanisms of relativistic electrons, as discussed in the previous section. The orbit has a low inclination of <10°, to make measurements near the equatorial plane of the magnetosphere.

The satellite is spin stabilized with a spin period of ∼4 s, giving a time resolution of 4 s for the measurements of three-dimensional particle distribution function. The satellite spin axis is directed toward the Sun, in order to reliably measure the electric field by using 40-m tip-to-tip antenna. The accurate measurement of electric field is also important to understand the particle acceleration mechanisms in the inner magnetosphere. The satellite has thrusters for initial operation, antenna extension, and to keep the spin axis toward the Sun. The weight and power consumption of the scientific instruments are estimated to be 40 kg and 50 W, respectively. The data production rate will be ∼40 kbps, which requires a telemetry rate of ∼0.5 Mbps for 2 h data transfer per day for 100% data coverage. Because the low gain antenna (LGA) in Fig. 4 can not transfer data in such a high rate, collaborations with several ground antennas will be necessary to increase the data transfer interval.

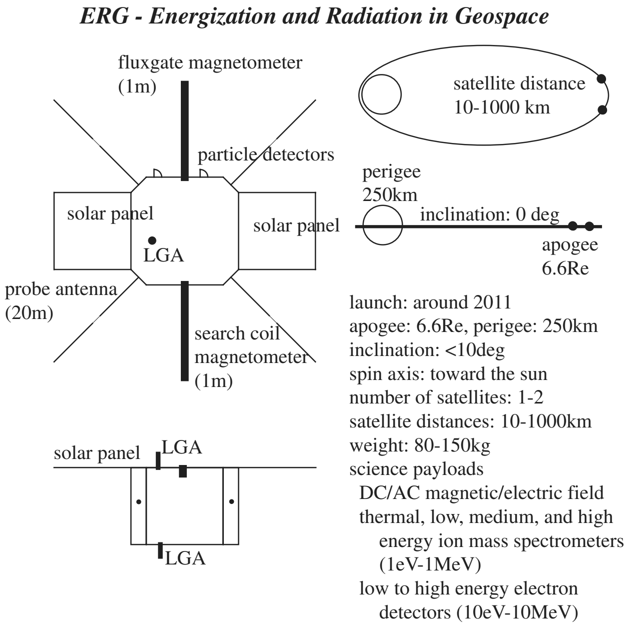

launch: around 2011
apogee: 6.6Re, perigee: 250km
inclination: <10deg
spin axis: toward the sun
number of satellites: 1-2
satellite distances: 10-1000km
weight: 80-150kg
science payloads
DC/AC magnetic/electric field
thermal, low, medium, and high energy ion mass spectrometers (1eV-1MeV)
low to high energy electron detectors (10eV-10MeV)

Fig. 4. Parameters of the ERG satellites, their orbit, and scientific payloads.

There is a possibility to split the ERG satellite into two small satellites. In case of two satellites, the size of each satellite (∼80 kg) may be smaller than that of single satellite (∼150 kg) and may be not affordable to have all the comprehensive instruments on board. In that case, some common instruments, such as magnetometers, wire antennas, and some particle detectors, will be put into both satellites, and the rest of the particle detectors may be separated into the two satellites. The two satellites will be put into the same orbit using one launcher, with distances from 10 (initial) to 1000 km (final) in order to measure the spatial extent and propagation of plasma/ULF waves and MHD scale disturbances. For high-energy particles, such a small distance does not make difference, so that the two satellites can be considered as one set of comprehensive instruments. If all the comprehensive instruments can be put into the two satellites, it will be better to place them into the different longitudinal sectors in the equatorial plane, in order to obtain better longitudinal coverage to trace the drifting particles.

References

Baker, D.N., Pulkkinen, T.I., Angelopoulos, V., Baumjohann, W., Mcpherron, R.L. Neutral line model of substorms: past results and present view. J. Geophys. Res. 101, 12,975, 1996.

Burch, J.L. IMAGE mission overview. Space Sci. Rev. 91, 1, 2000.

C:son Brandt, P., Ohtani, S., Mitchell, D.G., Fok, M.-C., Roelof, E.C., Demajistre, R. Global ENA observations of the storm mainphase ring current: Implications for skewed electric fields in the inner magnetosphere. Geophys. Res. Lett. 29 (20), 1954, doi:10.1029/2002GL015160, 2002.

Craven, P.D., Gallagher, D.L., Comfort, R.H. Relative concentration of He+ in the inner magnetosphere as observed by the DE 1 retarding ion mass spectrometer. J. Geophys. Res. 102, 2279, 1997.

Daglis, I.A. The role of magnetosphere–ionosphere coupling in magnetic storm dynamics, in: Magnetic Storms, AGU Monograph 98, pp. 107–116, AGU, Washington, DC, 1997.

Desorgher, L., Buhler, P., Zehnder, A., Fluckiger, E.O. Simulation of the outer radiation belt electron flux decrease during the March 26, 1995, magnetic storm. J. Geophys. Res. 105, 21211, 2000.

Ebihara, Y., Ejiri, M. Simulation study on the fundamental property of the storm-time ring current. J. Geophys. Res. 105, 15,843, 2000.

Ebihara, Y., Ejiri, M., Nilsson, H., Sandahl, I., Milillo, A., Grande, M., Fennell, J.F., Roeder, J.L. Statistical distribution of the storm-time proton ring current: POLAR measurements. Geophys. Res. Lett. 29, 1969, doi:10.1029/2002GL015430, 2002.

Ejiri, M., Hoffman, R.A., Smith, P.H. Energetic particle penetrations into the inner magnetosphere, NASA GSFC, X-625-77-254, 1977.

Elkington, S.R., Hudson, M.K., Chan, A.A. Acceleration of relativistic electrons via drift-resonant interaction with toroidal-mode Pc5 ULF oscillations. Geophys. Res. Lett. 26, 3273, 1999.

Frank, L.A. On the extraterrestrial ring current during geomagnetic storms. J. Geophys. Res. 72, 3753, 1967.

Fujimoto, M., Nishida, A. Energization and anisotropization of energetic electrons in the Earth's radiation belt by the recirculation process. J. Geophys. Res. 95, 4265, 1990.

Haerendel, G. Outstanding issues in understanding the dynamics of the inner plasma sheet and ring current during storms and substorms. Adv. Space Res. 25, 2379, 2000.

Horne, R.B., Thorne, R.M. Potential waves for relativistic electron scattering and stochastic acceleration during magnetic storms. Geophys. Res. Lett. 25, 3011, 1998.

Jordanova, V., Torbert, R., Thorne, R., Collin, H., Roeder, J., Foster, J. Ring current activity during the early Bz 0 phase of the January 1997 magnetic cloud. J. Geophys. Res. 104 (A11), 24,895–24,914, 1999.

Kepko, L., Kivelson, M. Generation of Pi 2 pulsations by bursty bulk flows. J. Geophys. Res. 104, 25,021, 1999.

Korth, A., Friedel, R., Mouikis, C., Fennell, J., Wygant, J., Korth, H. Comprehensive particle and field observations of magnetic storms at different local times from the CRRES spacecraft. J. Geophys. Res. 105 (A8), 18,729–18,740, 2000.

Kozyra, J.U., Fok, M.-C., Sanchez, E.R., Evans, D.S., Hamilton, D.C., Nagy, A.F. The role of precipitation losses in producing the rapid early recovery phase of the great magnetic storm of February 1986. J. Geophys. Res. 103, 6801, 1998.

Li, X., Baker, D.N., Temerin, M., Cayton, T.E., Reeves, G.D., Christensen, R.A., Blake, J.B., Looper, M.D., Nakamura, R., Kanekal, S.G. Multisatellite observations of the outer zone electron variation during the November 3–4, 1993, magnetic storm. J. Geophys. Res. 102, 14,123, 1997.

Liemohn, M., Kozyra, J., Thomsen, M., Roeder, J., Lu, G., Borovsky, J., Cayton, T. Dominant role of the asymmetric ring current in producing the stormtime *Dst**. J. Geophys. Res. 106 (A6), 10,883–10,904, 2001.

Liu, W.W., Rostoker, G., Baker, D.N. Internal acceleration of relativistic electrons by large-amplitude ULF pulsations. J. Geophys. Res. 104, 17391–17408, 1999.

Lui, A.T.Y. A synthesis of magnetospheric substorm models. J. Geophys. Res. 96, 1849, 1991.

Lui, A.T.Y. Inner magnetospheric plasma pressure distribution and its local time asymmetry. Geophys. Res. Lett. 30 (16), 1846, doi:10.1029/2003GL017596, 2003.

Lyons A new theory for magnetospheric substorms. J. Geophys. Res. 100, 19,069, 1995.

Miyoshi, Y., Morioka, A., Obara, T., Misawa, H., Nagai, T., Kasahara, Y. Rebuilding process of the outer radiation belt during the November 3, 1993, magnetic storm, NOAA and EXOS-D observations, J. Geophys. Res., doi:10.1029/2001ja007542, 2003.

Nagai, T. Space weather forecast: Prediction of relativistic electron intensity at synchronous orbit. Geophys. Res. Lett. 15, 425, 1988.

Obara, T., Miyoshi, Y., Morioka, A. Large enhancement of the outer belt electrons during magnetic storms. Earth Planets Space 53, 1163, 2001.

Olson, J.V. Pi 2 pulsations and substorm onsets: A review. J. Geophys. Res. 104, 17,499, 1991.

Oya, H. Studies on plasma and plasma waves in the plasmasphere and auroral particle acceleration region, by PWS on board the EXOS-D (Akebono) satellite. J. Geomagn. Geoelectr. 43 (Suppl.), 369, 1991.

Oya, H., Iizima, M., Morioka, A. Plasma turbulence disc circulating the equatorial region of the plasmasphere identified by the plasma wave detector (PWS) onboard the Akebono (EXOS-D) satellite. Geophys. Res. Lett. 18, 329, 1991.

Oya, H. Dynamical variation of plasmasphere revealed by PWS data onboard the Akebono (EXOS-D) satellite. J. Geomagn. Geoelectr. 49, S159, 1997.

Rowland, D.E., Wygant, J.R. Dependence of the large-scale, inner magnetospheric electric field on geomagnetic activity. J. Geophys. Res. 103, 14,959–14,964, 1998.

Sandel, B.R., King, R.A., Forrester, W.T., Gallagher, D.L., Broadfoot, A.L., Curtis, C.C. Initial results from the IMAGE extreme ultraviolet imager. Geophys. Res. Lett. 28, 1439, 2001.

Shiokawa, K., Yumoto, K., Newell, P.T., Meng, C.-I. Broadband electrons observed by the DMSP satellites during storm-time substorms. Geophys. Res. Lett. 23, 2529, 1996.

Shiokawa, K., Meng, C.I., Reeves, G.D., Rich, F.J., Yumoto, K. A multievent study of broadband electrons observed by the DMSP satellites and their relation to red aurora observed at midlatitude stations. J. Geophys. Res. 102, 14,237, 1997.

Shiokawa, K. et al. High-speed ion flow, substorm current wedge, and multiple Pi 2 pulsations. J. Geophys. Res. 103, 4491, 1998.

Shiokawa, K., Anderson, R.R., Daglis, W.J., Hughes, I.A., Wygant, J.R. Simultaneous DMSP and CRRES observation of broadband electrons during a storm-time substorm on March 25, 1991. Phys. Chem. Earth 24, 281, 1999.

Summers, D., Ma, C. A model for generating relativistic electrons in the Earth's inner magnetosphere based on gyroresonant wave–particle interactions. J. Geophys. Res. 105, 2625, 2000a.

Summers, D., Ma, C. Rapid acceleration of electrons in the magnetosphere by fastmode MHD waves. J. Geophys. Res. 105, 15,887, 2000b.

Takahashi, K., Ohtani, S.-I., Hughes, W.J., Anderson, R.R. CRRES observation of Pi 2 pulsations: Wave mode inside and outside the plasmasphere. J. Geophys. Res. 106, 15,561, 2001.

Tan, L., Fung, S., Shao, X. Observation of magnetospheric relativistic electrons accelerated by Pc-5 ULF waves. Geophys. Res. Lett., 31, doi:10.1029/2004GL019459, 2004.

Yumoto, K.and the CPMN group Characteristics of Pi 2 magnetic pulsations observed at the CPMN stations: A review of the STEP results. Earth Planets Space 53, 981, 2001.